

Supporting Information for

Interaction of bi-nuclear gallium(III) complexes with human serum albumin and impact on potency towards osteosarcoma stem cells

Xiao Feng ^a and Kogularamanan Suntharalingam ^{*a}

^aSchool of Chemistry, University of Leicester, Leicester, LE1 7RH, United Kingdom.

Email: k.suntharalingam@leicester.ac.uk

Table of Content

Experimental Details

- Figure S1.** (A) Representative emission spectra of HSA (1 μM) upon addition of aliquots of **5** (up to 30 μM). (B) I^0/I versus $[Q]$ plot corresponding to the emission data for HSA (1 μM) upon addition of **5**. The gradient was used to calculate the quenching constant (K_q).
- Figure S2.** (A) Representative emission spectra of HSA (1 μM) upon addition of aliquots of **6** (up to 30 μM). (B) I^0/I versus $[Q]$ plot corresponding to the emission data for HSA (1 μM) upon addition of **6**. The gradient was used to calculate the quenching constant (K_q).
- Figure S3.** (A) Representative emission spectra of HSA (1 μM) upon addition of aliquots of **7** (up to 15 μM). (B) I^0/I versus $[Q]$ plot corresponding to the emission data for HSA (1 μM) upon addition of **7**. The gradient was used to calculate the quenching constant (K_q).
- Figure S4.** (A) UV-vis spectra of HSA (40 μM), **4** (40 μM), or HSA (40 μM) + **4** (40 μM) in water:DMSO (250:1). (B) UV-vis spectra of HSA (40 μM), **5** (40 μM), or HSA (40 μM) + **5** (40 μM) in water:DMSO (250:1). (C) UV-vis spectra of HSA (40 μM), **6** (40 μM), or HSA (40 μM) + **6** (40 μM) in water:DMSO (250:1). (D) UV-vis spectra of HSA (40 μM), **7** (40 μM), or HSA (40 μM) + **7** (40 μM) in water:DMSO (250:1).
- Figure S5.** $\text{Log}[I^0/I - 1]$ versus $\text{Log}[Q]$ plots corresponding to the emission data for HSA (1 μM) upon addition of (A) **4** (up to 30 μM), (B) **5** (up to 30 μM), (C) **6** (up to 30 μM) or **7** (up to 15 μM). The y-intercept was used to calculate the binding constant (K_a) and the gradient was used to calculate the number of binding sites (n).
- Figure S6.** Job plots for the binding of (A) **4**, (B) **5**, (C) **6** or (D) **7** to HSA indicating 1:1 or 4:3 stoichiometry.
- Figure S7.** Representative synchronous fluorescence spectra of HSA (1 μM) upon addition of aliquots of **4** (up to 5 μM) where $\Delta\lambda = 15$ or 60 nm.
- Figure S8.** Representative synchronous fluorescence spectra of HSA (1 μM) upon addition of aliquots of **5** (up to 5 μM) where $\Delta\lambda = 15$ or 60 nm.

- Figure S9.** Representative synchronous fluorescence spectra of HSA (1 μM) upon addition of aliquots of **6** (up to 5 μM) where $\Delta\lambda = 15$ or 60 nm.
- Figure S10.** Representative synchronous fluorescence spectra of HSA (1 μM) upon addition of aliquots of **7** (up to 5 μM) where $\Delta\lambda = 15$ or 60 nm.
- Table S1.** % Decrease in emission intensity in synchronous fluorescence spectra of HSA (1 μM) upon addition of aliquots of **4-7** (up to 5 μM) where $\Delta\lambda = 15$ or 60 nm.
- Figure S11.** (A) Image of **4** interacting with HSA within subdomain IIA (Sudlow site I) and relative distance from Trp214. (B) Image of **5** interacting with HSA within subdomain IIA (Sudlow site I) and relative distance from Trp214.
- Figure S12.** HSA (5 μM) resolved by 4-20 % SDS-PAGE gel electrophoresis and stained by Coomassie Blue G-250 in the absence and presence of **4-7** (5 μM) after incubation at 37 $^{\circ}\text{C}$ for 24 h. Lane 1: Protein ladder, Lane 2: HSA only; Lane 3-6: HSA (5 μM) + **4-7** (5 μM).
- Figure S13.** (A) Dynamic light scattering size distribution of HSA (100 μM) suspended in PBS. (B) Dynamic light scattering size distribution of HSA (100 μM) in the presence of **5** (100 μM) suspended in PBS. Size refers to diameter in nm.
- Figure S14.** TEM images of (A) HSA (100 μM) suspended in water and (B) HSA (100 μM) in the presence of **5** suspended in water.
- Figure S15.** Images of various water:DMSO (200:1) solutions of **4** (13-500 μM) and HSA-**4** (500 μM).
- Figure S16.** Images of various water:DMSO (200:1) solutions of **5** (13-500 μM) and HSA-**5** (500 μM).
- Figure S17.** Images of various water:DMSO (200:1) solutions of **6** (13-500 μM) and HSA-**6** (500 μM).
- Figure S18.** Images of various water:DMSO (200:1) solutions of **7** (13-500 μM) and HSA-**7** (500 μM).
- Figure S19.** Representative dose-response curves for the treatment of U2OS cells with (A) HSA-**4**, (B) HSA-**5**, (C) HSA-**6** or (D) HSA-**7** after 72 h incubation.
- Figure S20.** Representative dose-response curves for the treatment of U2OS-MTX cells with (A) HSA-**4**, (B) HSA-**5**, (C) HSA-**6** or (D) HSA-**7** after 72 h incubation.
- Table S2.** Reported IC_{50} values for **4-7** against U2OS and U2OS-MTX cells. Determined after 72 h incubation (mean of three independent experiments \pm SD).
- Figure S21.** Representative dose-response curves for the treatment of (A) U2OS cells or (B) U2OS-MTX cells with HSA after 72 h incubation.
- Figure S22.** Representative bright-field images ($\times 10$) of U2OS-MTX sarcospheres in the absence and presence of salinomycin at its IC_{20} values for 10 days.
- Figure S23.** Representative dose-response curves for the treatment of U2OS-MTX sarcospheres with HSA-**4-7** after 10 days incubation.

References

Experimental Details

Materials and Methods. The binuclear gallium(III) complexes **4-7** were prepared according to our previously reported protocols.¹ The HSA-bound binuclear gallium(III) complexes HSA-**4-7** were prepared by incubated binuclear gallium(III) complexes **4-7** with HSA in water (1:1 molar ratio, 30 min). The fluorescence studies were performed on a Varian Cary Eclipse spectrometer.

Human Serum Albumin Fluorescence Studies. To HSA (1 μ M) in 5 mM Tris-HCl (pH 7.4) buffer, an increasing amount of the binuclear gallium(III) complexes **4-7** (0-30 μ M) was added. The emission spectrum was recorded between 300 and 450 nm with an excitation wavelength of 280 nm. The fluorescence intensity at *ca.* 340 nm was used to determine the quenching constant (K_q), bimolecular quenching rate constant (k_q), binding constant (K_a), and the number of binding sites (n) of binuclear gallium(III) complexes **4-7**. The synchronous fluorescence spectra were measured at $\Delta\lambda = 15$ nm and 60 nm.

The quenching constant (K_q) was determined using the Stern-Volmer equation: $I^0/I = K_q[Q] + 1$, where I^0 is the emission intensity of HSA in the absence of **4-7**, I is the emission intensity of HSA upon addition of **4-7**, K_q is the quenching constant, and $[Q]$ is the concentration of **4-7**. The quenching constants (K_q) were extrapolated from I^0/I versus $[Q]$ plots. The bimolecular quenching rate constant (k_q) was determined from the following equation: $k_q = K_q / \tau_0$, where k_q is the bimolecular quenching rate constant, K_q is the quenching constant, and τ_0 is the average lifetime of HSA fluorescence in the absence of the quencher. The τ_0 of HSA is 5.71×10^{-9} s.^{2,3}

The binding constant (K_a) of binuclear gallium(III) complexes **4-7** to HSA and the number of binding sites (n) were determined using the modified Stern-Volmer equation: $\log[I^0/I - 1] = \log(K_a) + n\log[Q]$, where I^0 is the emission intensity of HSA in the absence of **4-7**, I is the emission intensity of HSA upon addition of **4-7**, $[Q]$ is the concentration of **4-7**, and n is to the number of binding sites. The K_a and n values were extrapolated from $\log[I^0/I - 1]$ versus $\log[Q]$ plots.

Human Serum Albumin Job Plots from Fluorescence Spectroscopy. A series of solutions containing binuclear gallium(III) complexes **4-7** and HSA were prepared such that the sum of their concentrations remained constant (2 μ M). The molar fraction of 11 samples was varied from 0.1 to 1.0, and $(I_0 - I) \times M_{\text{HSA}}$ was plotted against the molar fraction of **4-7**, where I_0 is the fluorescent signal of HSA integrated from 300 nm to 450 nm with excitation at 280 nm, I is that of the mixture of HSA and **4-7**, and M_{HSA} is the molar fraction of HSA.

Molecular Docking Analysis. Docking studies were carried out using Autodock 4.0. The protein structure used was crystallographically determined and retrieved from the Protein Data Bank (HSA bound to myristic acid and the *R*-(+) enantiomer of warfarin; 1H9Z).⁴ The previously resolved X-ray structures of binuclear gallium(III) complexes **4** and **5** were used for docking studies.¹ Protein structures were modified to include polar hydrogen atoms. During docking studies, the protein structure was kept rigid. Rotation in the binuclear gallium(III) complexes **4** and **5**, was permitted about all single bonds.

Human Serum Albumin Gel Electrophoresis Studies. To HSA (5 μ M) in 5 mM Tris-HCl (pH 7.4) buffer, the binuclear gallium(III) complexes **4-7** were added and incubated at 37 °C for 24 h. Bromophenol blue was added to the samples and loaded onto a gel. The protein fragments were resolved by 4-20 % SDS-PAGE (150 V for 1 h). The protein bands were

visualised using Coomassie Blue G-250. The stained gel was imaged using the Bio-Rad ChemiDoc Imaging System.

Dynamic Light Scattering Studies. The size distribution and polydispersity of HSA (100 μM) alone or in the presence of **5** (100 μM) in PBS (pH 7.4) was obtained by loading the solutions into disposable micro-cuvettes and measuring the dynamic light scattering (DLS) of the solution using a Zetasizer Nanoseries spectrometer (Malvern).

Transmission Electron Microscopy. An aliquot of HSA (100 μM) or HSA (100 μM) in the presence of **5** in MilliQ water was allowed to evaporate on a square glass slide and stained with uranyl acetate. Imaging was conducted using a JEOL 2100 Transmission Electron Microscope within the University of Leicester Electron Microscopy Facility (EMF).

Cell Lines and Cell Culture Conditions. The U2OS bone osteosarcoma cell line was acquired from American Type Culture Collection (ATCC, Manassas, VA, USA) and cultured in Dulbecco's Modified Eagle's Medium (DMEM) supplemented with 10% fetal bovine serum and 1% penicillin. The cells were grown at 310 K in a humidified atmosphere containing 5% CO_2 . To gain access to OSC-enriched cells, a full T75 flask of U2OS cells was treated with methotrexate (300 nM) for 4 days.⁵ The cells (labelled U2OS-MTX cells) were then used immediately.

Cytotoxicity MTT assay. The colourimetric MTT assay was used to determine the toxicity of test agents. U2OS and U2OS-MTX cells (5×10^3) were seeded in each well of a 96-well plate. After incubating the cells overnight, various concentrations of the HSA-bound binuclear gallium(III) complexes HSA-**4-7** (0.0004-100 μM) were added and incubated for 72 h (total volume 200 μL). After 72 h, 20 μL of a 4 mg/mL solution of MTT in PBS was added to each well, and the plate was incubated for an additional 4 h. The DMEM/MTT mixture was aspirated and 200 μL of DMSO was added to dissolve the resulting purple formazan crystals. The absorbance of the solutions in each well was read at 550 nm. Absorbance values were normalised to untreated control wells and plotted as concentration of test agent versus % cell viability. IC_{50} values were interpolated from the resulting dose dependent curves. The reported IC_{50} values are the average of three independent experiments, each consisting of six replicates per concentration level (overall $n = 18$).

Sarcosphere Formation and Viability Assay. U2OS-MTX cells (2.5×10^4) were plated in ultralow-attachment 96-well plates (Corning) and incubated in DMEM supplemented with N2 (Invitrogen), human EGF (10 ng/mL), and human bFGF (10 ng/mL) for 10 days. Studies were also conducted in the presence of the HSA-bound binuclear gallium(III) complexes HSA-**4-7** (0-133 μM). Sarcospheres treated with the HSA-bound binuclear gallium(III) complexes HSA-**4-7** (at their respective IC_{20} values, 10 days) were imaged using an inverted microscope. The viability of the sarcospheres was determined by addition of a resazurin-based reagent, TOX8 (Sigma). After incubation for 16 h, the fluorescence of the solutions was read at 590 nm ($\lambda_{\text{ex}} = 560$ nm). Viable sarcospheres reduce the amount of the oxidized TOX8 form (blue) and concurrently increases the amount of the fluorescent TOX8 intermediate (red), indicating the degree of sarcosphere cytotoxicity caused by the test agents. Fluorescence values were normalised to untreated controls and plotted as concentration of test agent versus % sarcosphere viability. IC_{50} values were interpolated from the resulting dose dependent curves. The reported IC_{50} values are the average of three independent experiments, each consisting of three replicates per concentration level (overall $n = 9$).

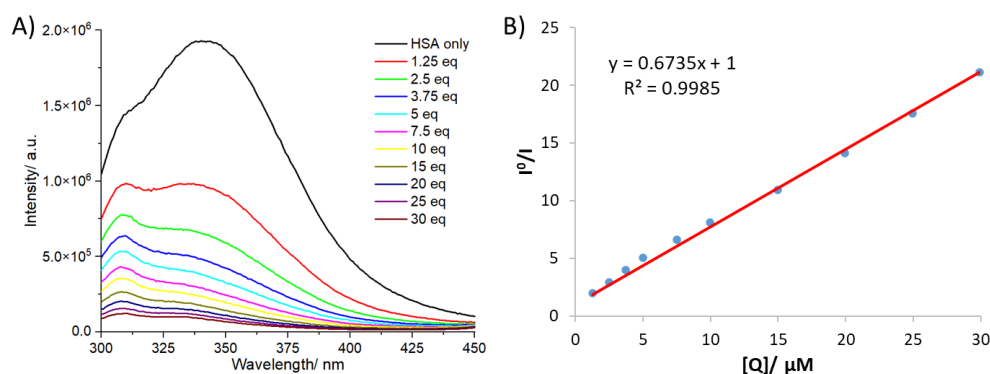


Figure S1. (A) Representative emission spectra of HSA (1 μM) upon addition of aliquots of **5** (up to 30 μM). (B) I^0/I versus $[Q]$ plot corresponding to the emission data for HSA (1 μM) upon addition of **5**. The gradient was used to calculate the quenching constant (K_q).

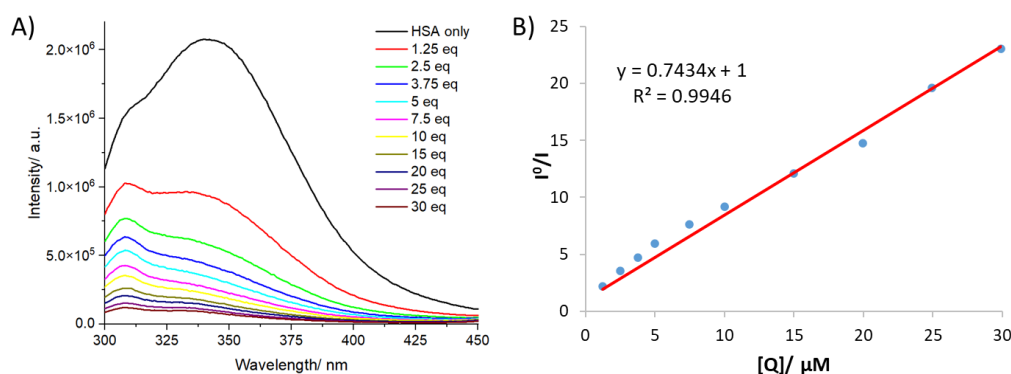


Figure S2. (A) Representative emission spectra of HSA (1 μM) upon addition of aliquots of **6** (up to 30 μM). (B) I^0/I versus $[Q]$ plot corresponding to the emission data for HSA (1 μM) upon addition of **6**. The gradient was used to calculate the quenching constant (K_q).

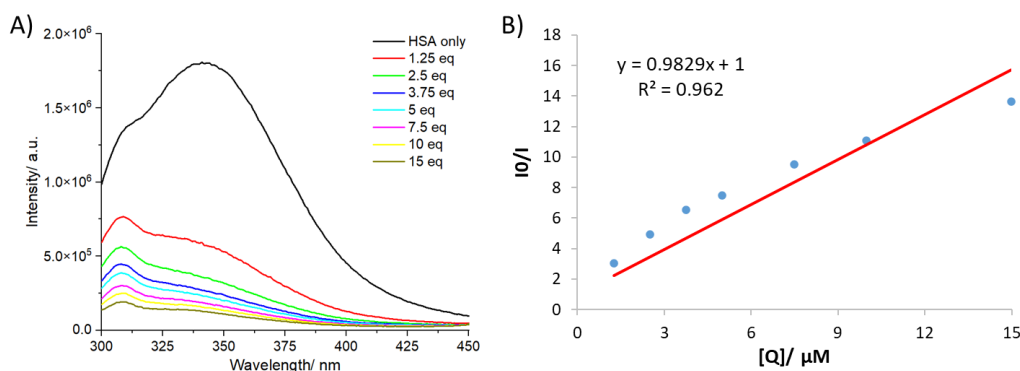


Figure S3. (A) Representative emission spectra of HSA (1 μM) upon addition of aliquots of **7** (up to 15 μM). (B) I^0/I versus $[Q]$ plot corresponding to the emission data for HSA (1 μM) upon addition of **7**. The gradient was used to calculate the quenching constant (K_q).

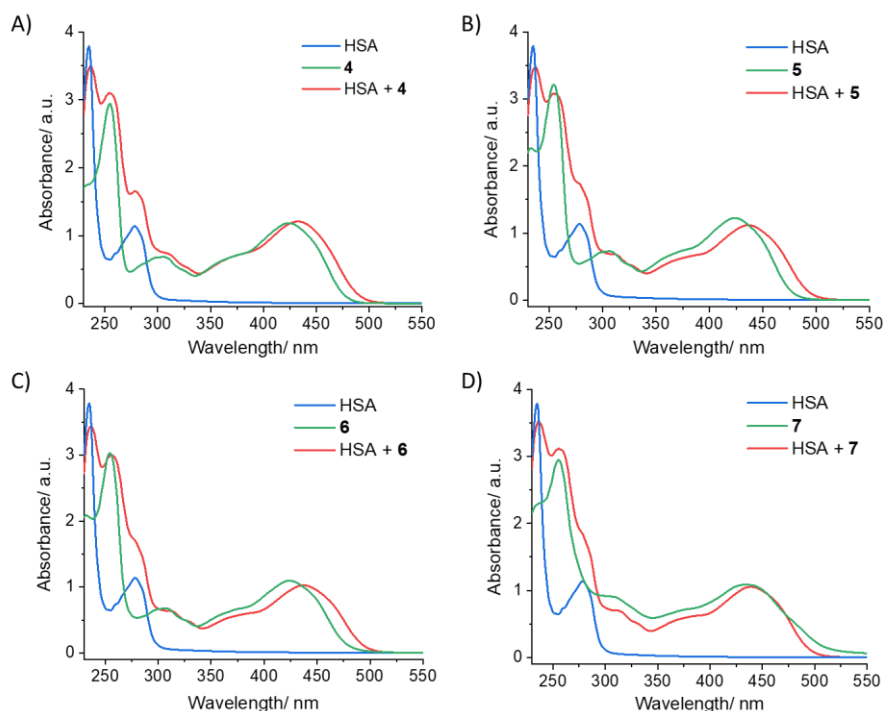


Figure S4. (A) UV-vis spectra of HSA (40 μM), **4** (40 μM), or HSA (40 μM) + **4** (40 μM) in water:DMSO (250:1). (B) UV-vis spectra of HSA (40 μM), **5** (40 μM), or HSA (40 μM) + **5** (40 μM) in water:DMSO (250:1). (C) UV-vis spectra of HSA (40 μM), **6** (40 μM), or HSA (40 μM) + **6** (40 μM) in water:DMSO (250:1). (D) UV-vis spectra of HSA (40 μM), **7** (40 μM), or HSA (40 μM) + **7** (40 μM) in water:DMSO (250:1).

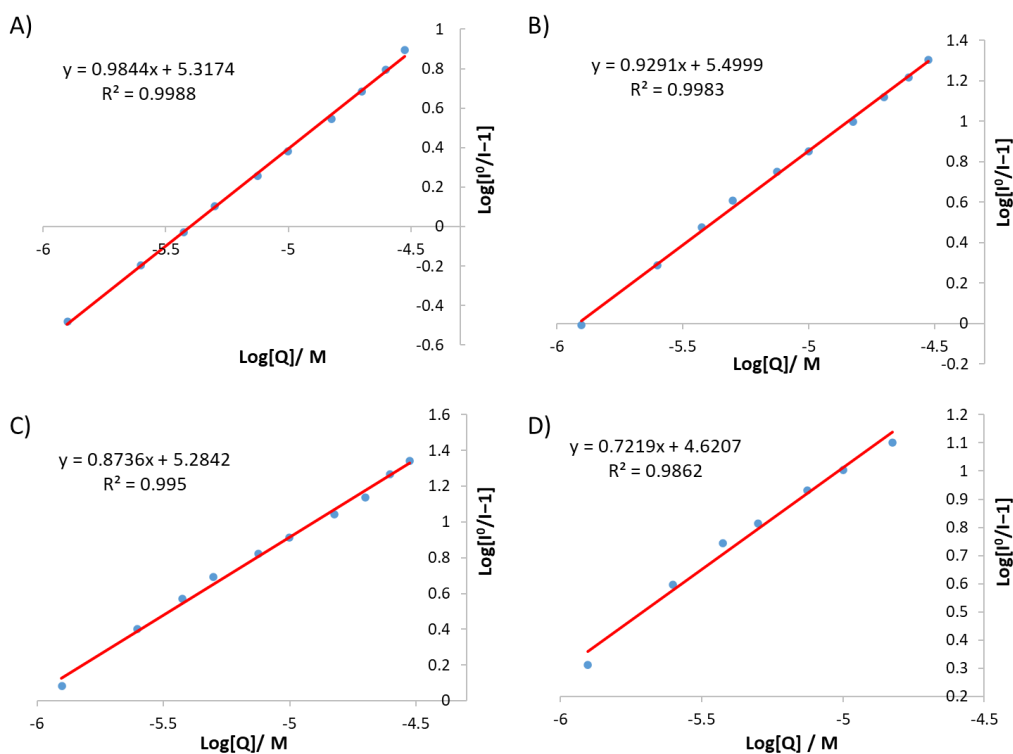


Figure S5. Log[I⁰/I - 1] versus Log[Q] plots corresponding to the emission data for HSA (1 μM) upon addition of (A) **4** (up to 30 μM), (B) **5** (up to 30 μM), (C) **6** (up to 30 μM) or **7** (up to 15 μM). The y-intercept was used to calculate the binding constant (K_a) and the gradient was used to calculate the number of binding sites (n).

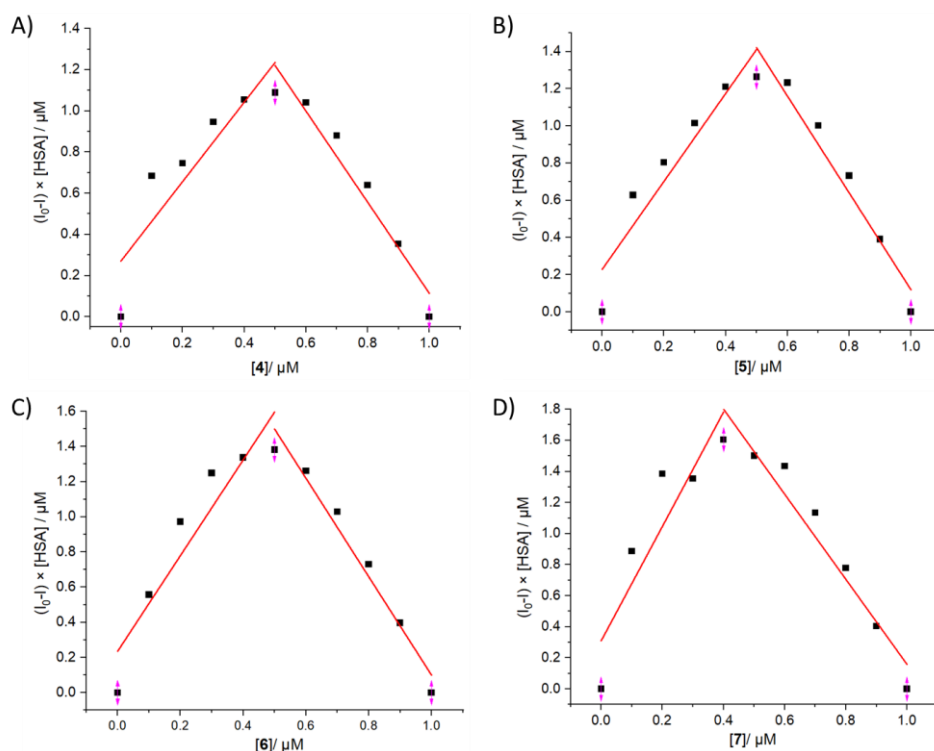


Figure S6. Job plots for the binding of (A) **4**, (B) **5**, (C) **6** or (D) **7** to HSA indicating 1:1 or 4:3 stoichiometry.

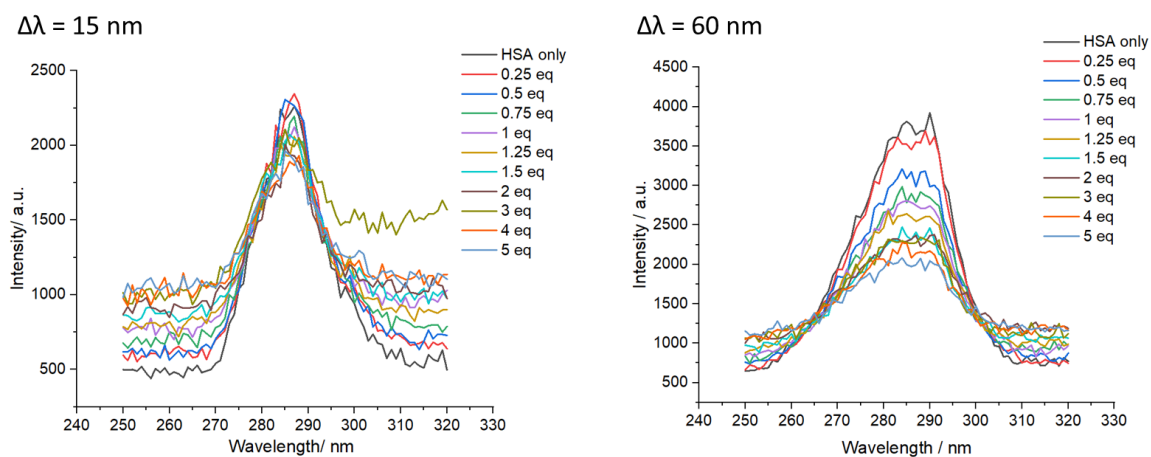


Figure S7. Representative synchronous fluorescence spectra of HSA (1 μM) upon addition of aliquots of **4** (up to 5 μM) where $\Delta\lambda = 15$ or 60 nm.

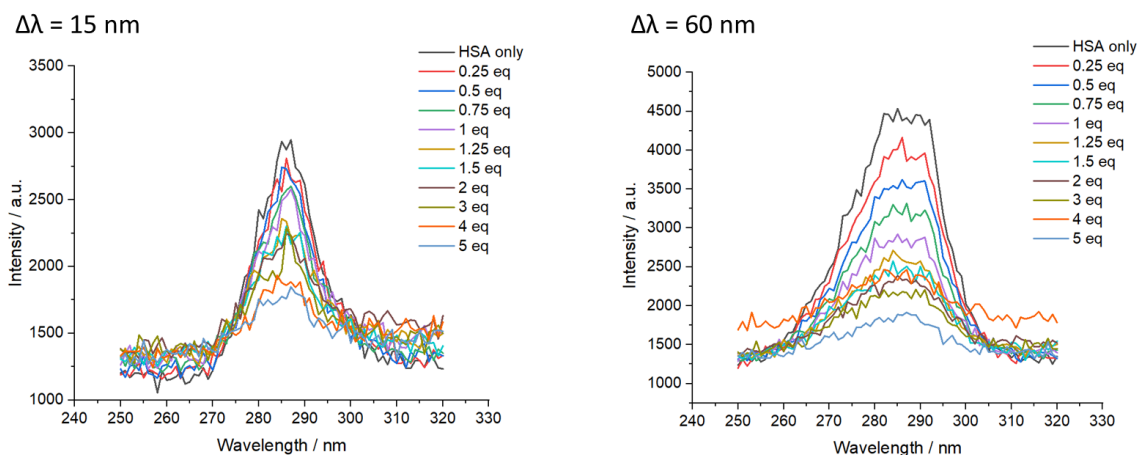


Figure S8. Representative synchronous fluorescence spectra of HSA (1 μM) upon addition of aliquots of 5 (up to 5 μM) where $\Delta\lambda = 15$ or 60 nm.

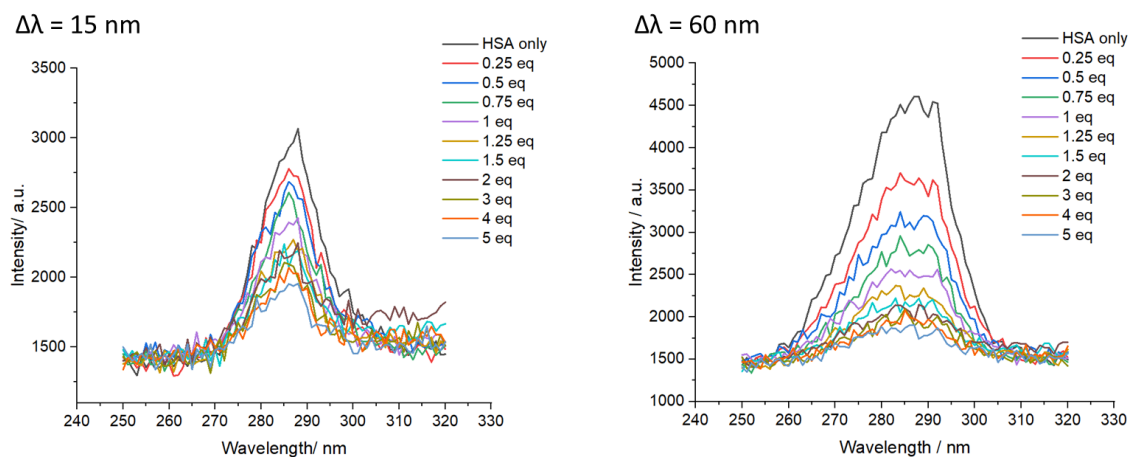


Figure S9. Representative synchronous fluorescence spectra of HSA (1 μM) upon addition of aliquots of 6 (up to 5 μM) where $\Delta\lambda = 15$ or 60 nm.

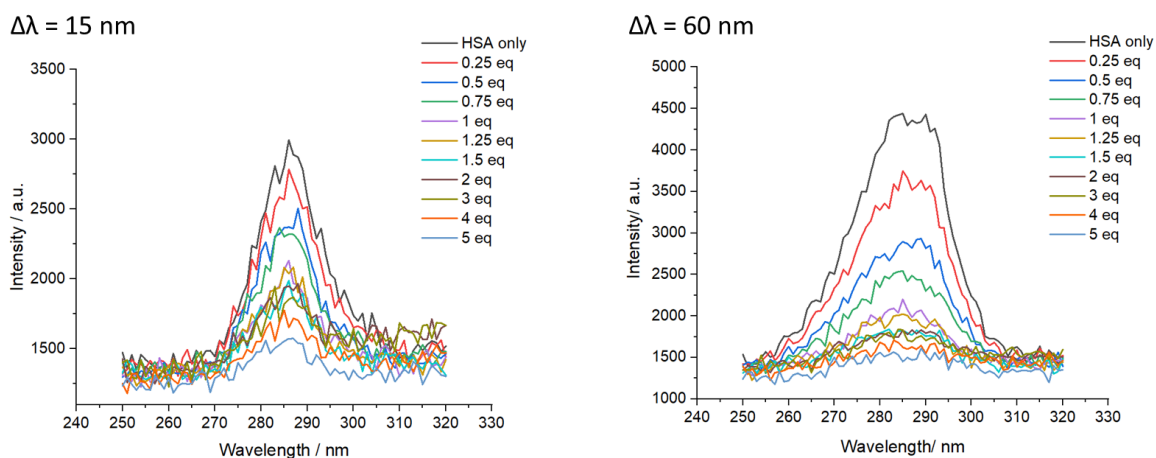


Figure S10. Representative synchronous fluorescence spectra of HSA (1 μM) upon addition of aliquots of 7 (up to 5 μM) where $\Delta\lambda = 15$ or 60 nm.

Table S1. % Decrease in emission intensity in synchronous fluorescence spectra of HSA (1 μM) upon addition of aliquots of **4-7** (up to 5 μM) where $\Delta\lambda = 15$ or 60 nm.

Ga(III) complex	$\Delta\lambda = 15$ nm	$\Delta\lambda = 60$ nm
4	21.8	57.3
5	63.7	81.1
6	64.5	85.8
7	81.1	94.1

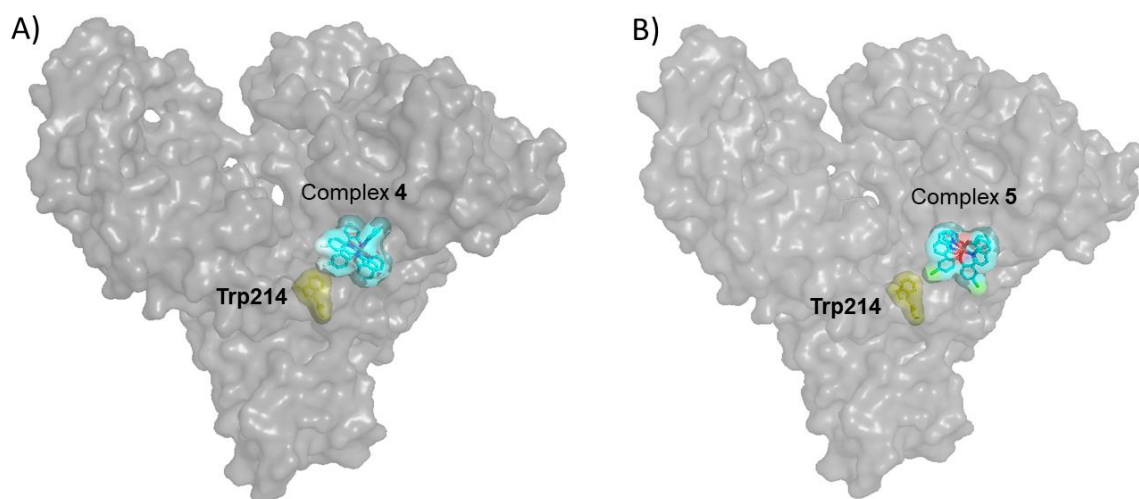


Figure S11. (A) Image of **4** interacting with HSA within subdomain IIA (Sudlow site I) and relative distance from Trp214. (B) Image of **5** interacting with HSA within subdomain IIA (Sudlow site I) and relative distance from Trp214.

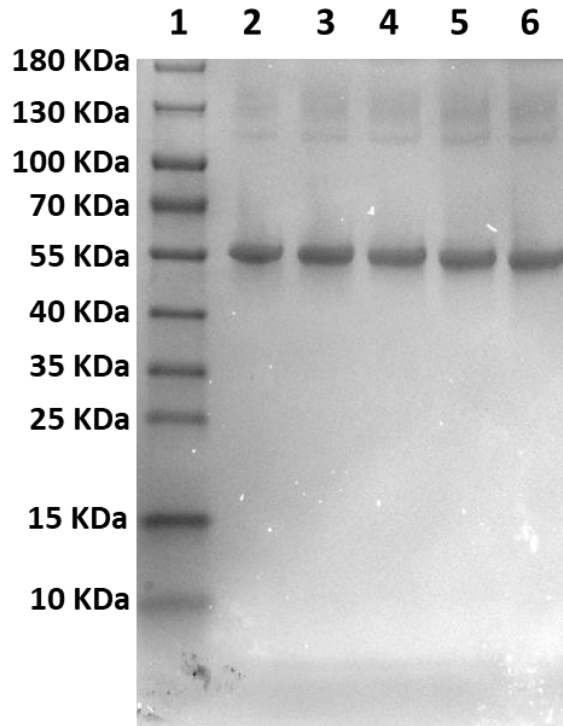


Figure S12. HSA (5 μM) resolved by 4-20 % SDS-PAGE gel electrophoresis and stained by Coomassie Blue G-250 in the absence and presence of **4-7** (5 μM) after incubation at 37 $^{\circ}\text{C}$ for 24 h. Lane 1: Protein ladder, Lane 2: HSA only; Lane 3-6: HSA (5 μM) + **4-7** (5 μM).

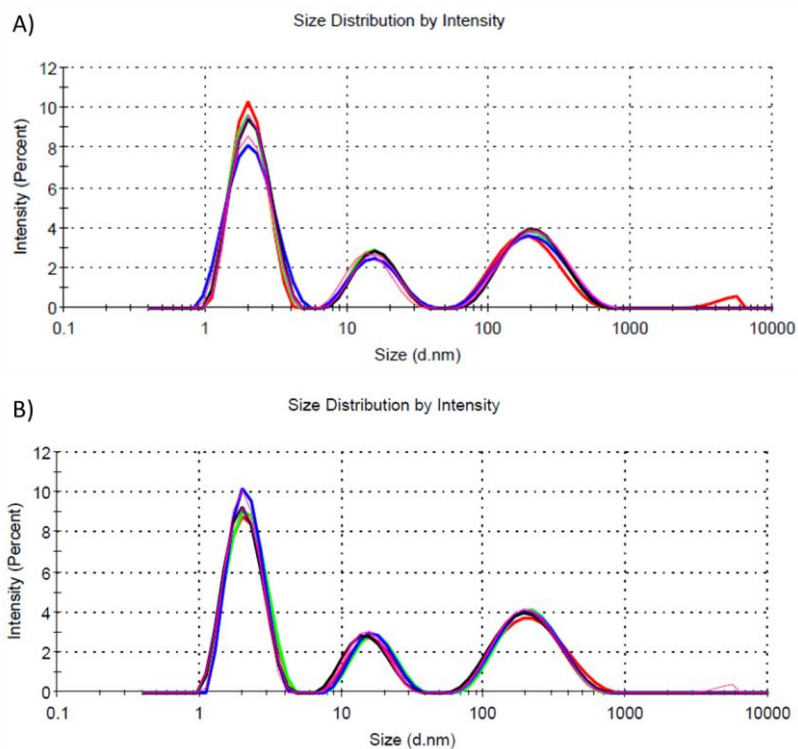


Figure S13. (A) Dynamic light scattering size distribution of HSA (100 μM) suspended in PBS. (B) Dynamic light scattering size distribution of HSA (100 μM) in the presence of **5** (100 μM) suspended in PBS. Size refers to diameter in nm.

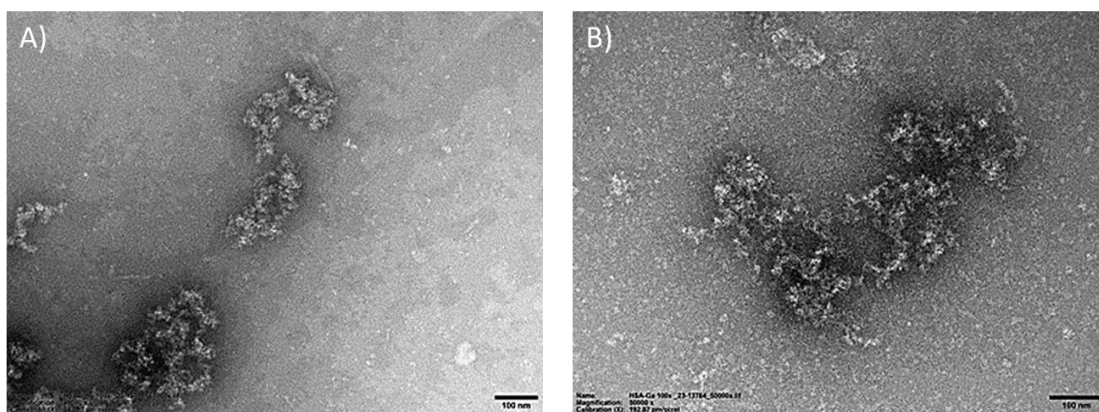


Figure S14. TEM images of (A) HSA (100 μM) suspended in water and (B) HSA (100 μM) in the presence of **5** suspended in water.

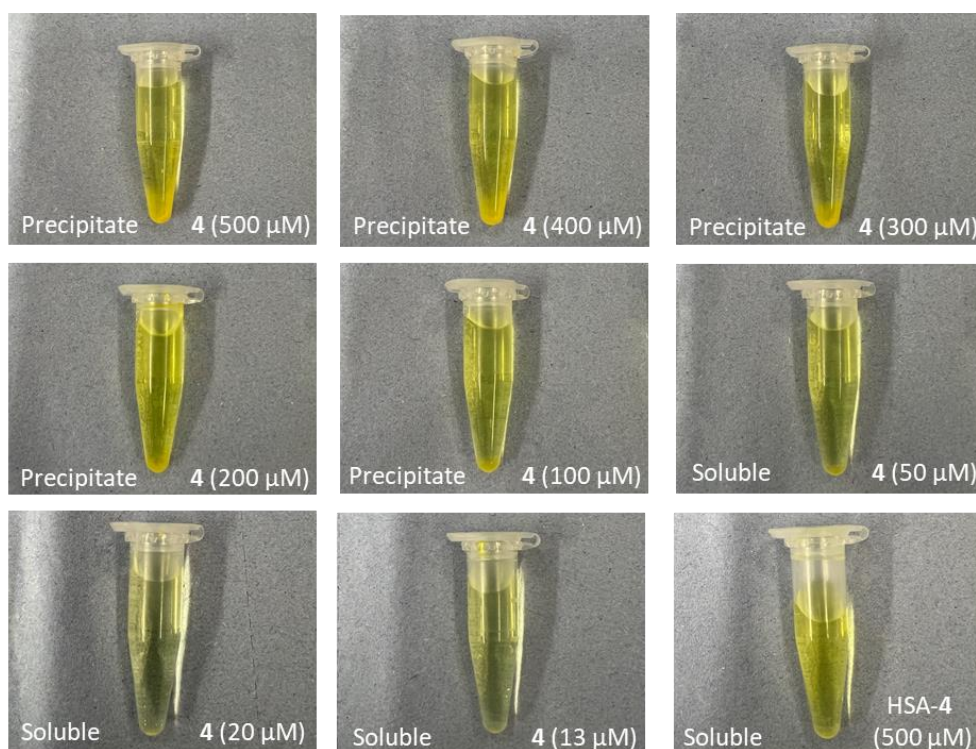


Figure S15. Images of various water:DMSO (200:1) solutions of **4** (13-500 μM) and HSA-4 (500 μM).

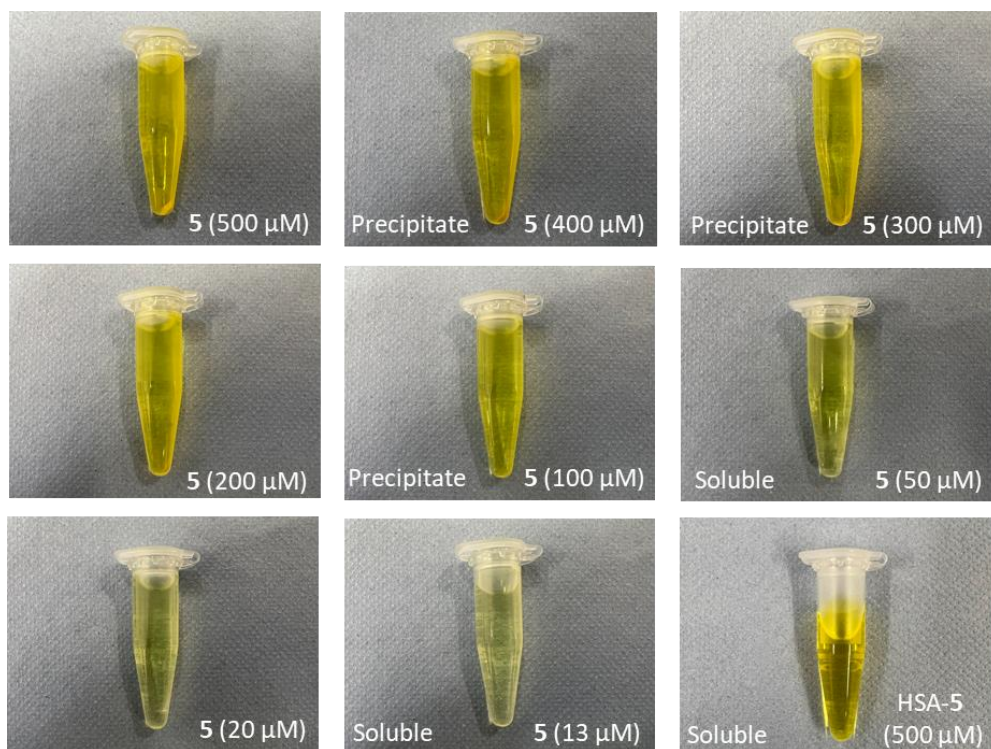


Figure S16. Images of various water:DMSO (200:1) solutions of **5** (13-500 μM) and HSA-**5** (500 μM).

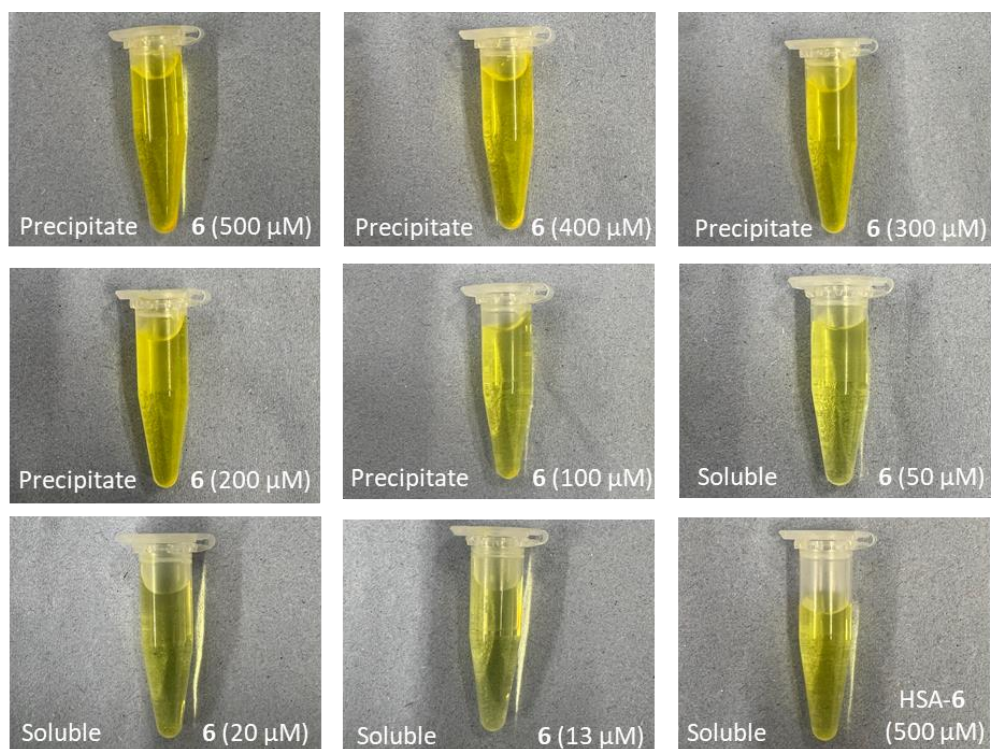


Figure S17. Images of various water:DMSO (200:1) solutions of **6** (13-500 μM) and HSA-**6** (500 μM).

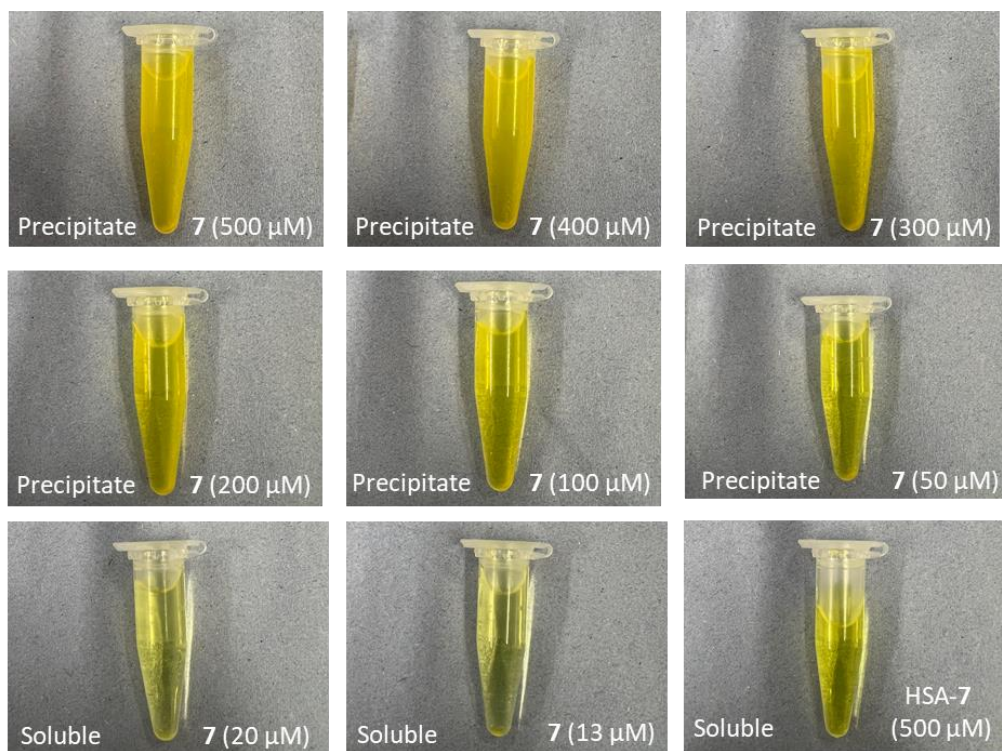


Figure S18. Images of various water:DMSO (200:1) solutions of **7** (13-500 μM) and HSA-7 (500 μM).

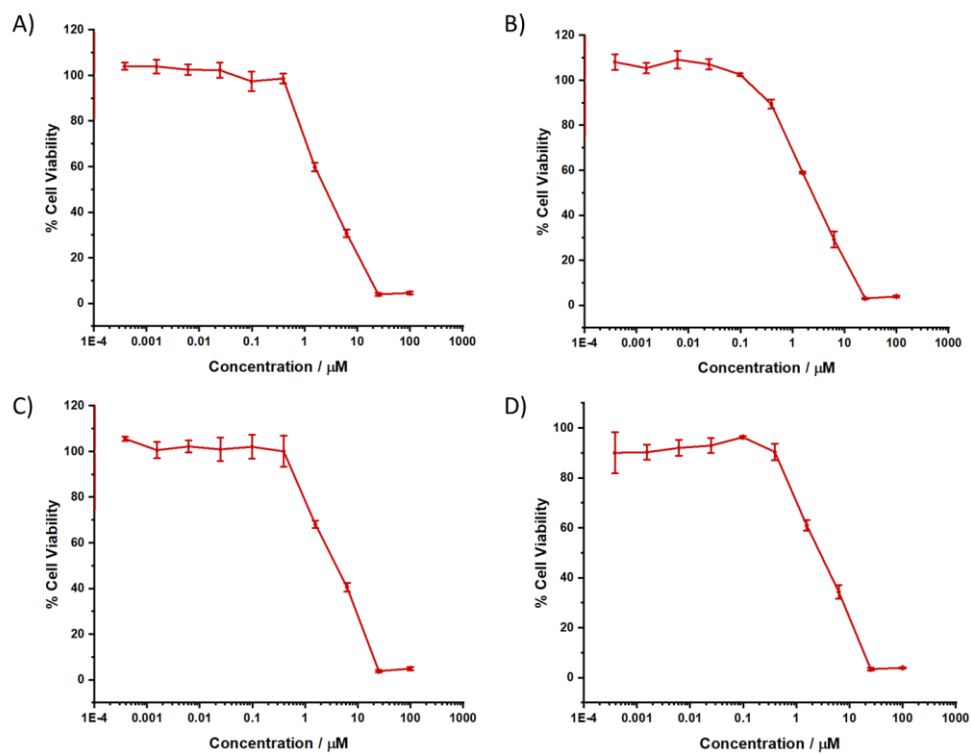


Figure S19. Representative dose-response curves for the treatment of U2OS cells with (A) HSA-4, (B) HSA-5, (C) HSA-6 or (D) HSA-7 after 72 h incubation.

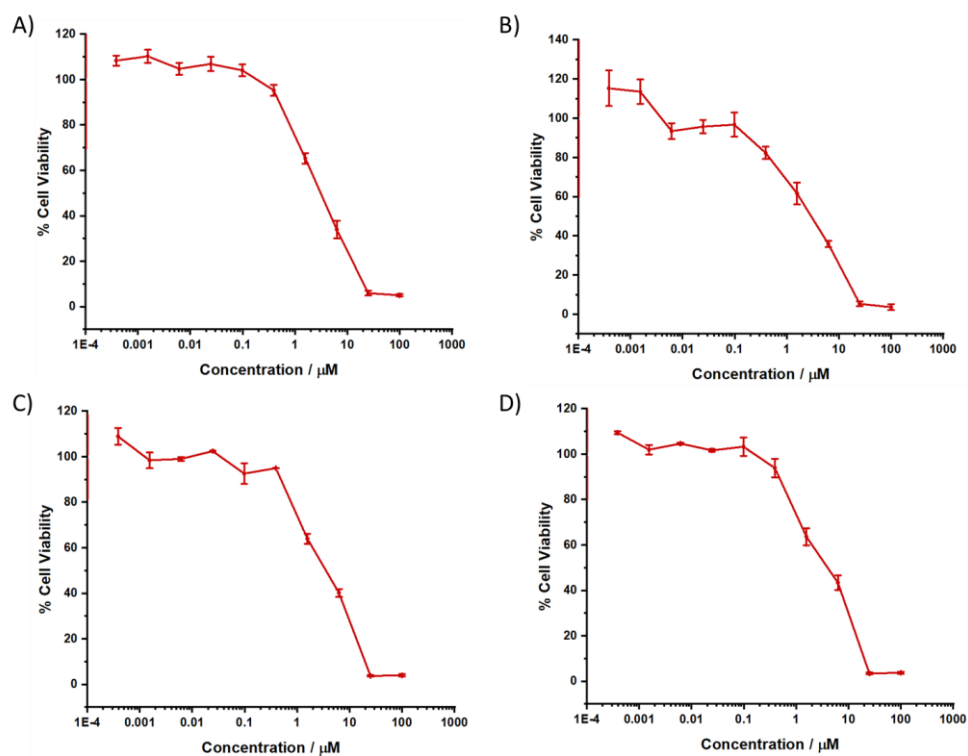


Figure S20. Representative dose-response curves for the treatment of U2OS-MTX cells with (A) HSA-4, (B) HSA-5, (C) HSA-6 or (D) HSA-7 after 72 h incubation.

Table S2. Reported IC_{50} values for 4-7 against U2OS and U2OS-MTX cells. Determined after 72 h incubation (mean of three independent experiments \pm SD).¹

Gallium(III) complex	U2OS [μM]	U2OS-MTX [μM]
4	5.71 ± 0.04	10.74 ± 0.39
5	4.10 ± 0.19	8.70 ± 0.38
6	5.07 ± 0.21	13.71 ± 0.01
7	4.93 ± 0.35	9.65 ± 0.83

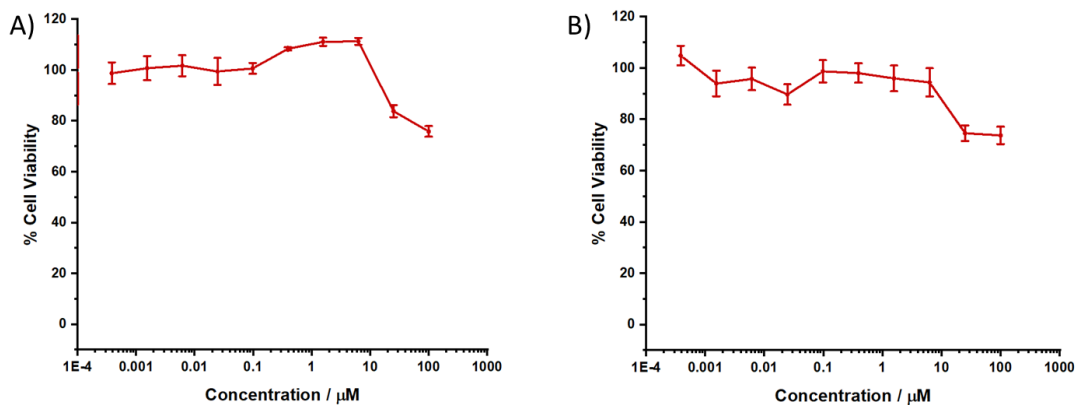


Figure S21. Representative dose-response curves for the treatment of (A) U2OS cells or (B) U2OS-MTX cells with HSA after 72 h incubation.

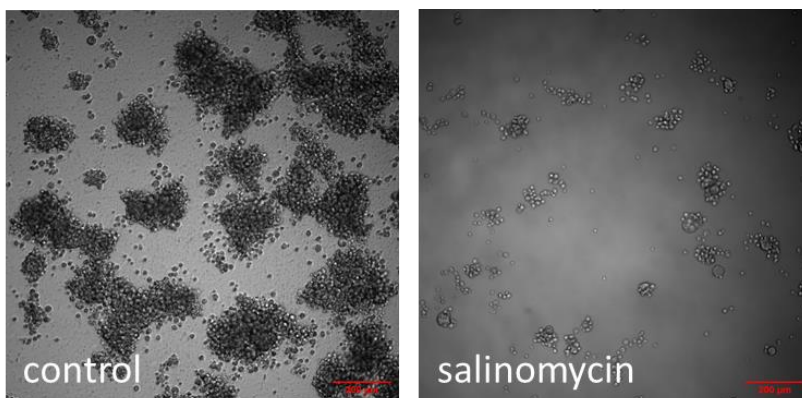


Figure S22. Representative bright-field images ($\times 10$) of U2OS-MTX sarcospheres in the absence and presence of salinomycin at its IC_{20} values for 10 days.

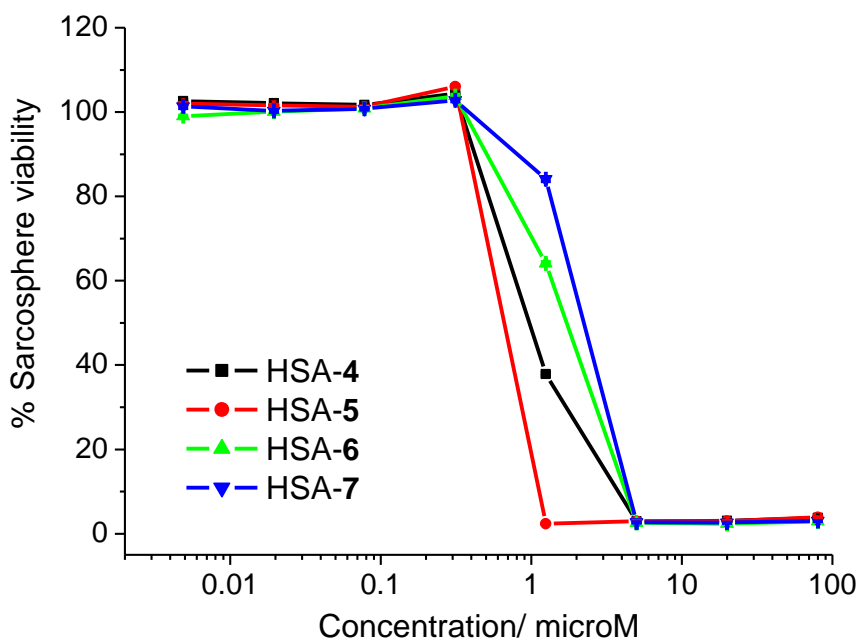


Figure S23. Representative dose-response curves for the treatment of U2OS-MTX sarcospheres with HSA-4-7 after 10 days incubation.

References

1. X. Feng, S. Dhandore, Y. Liu, K. Singh, F. Ortu and K. Suntharalingam, *Chem. Eur. J.*, 2025, **31**, e202500747.
2. W. R. Ware, *J. Phys. Chem.*, 1962, **66**, 455-458.
3. A. Hussain, M. F. AlAjmi, M. T. Rehman, S. Amir, F. M. Husain, A. Alsalme, M. A. Siddiqui, A. A. AlKhedhairy and R. A. Khan, *Sci. Rep.*, 2019, **9**, 5237.
4. I. Petitpas, A. A. Bhattacharya, S. Twine, M. East and S. Curry, *J. Biol. Chem.*, 2001, **276**, 22804-22809.
5. Q. L. Tang, Y. Liang, X. B. Xie, J. Q. Yin, C. Y. Zou, Z. Q. Zhao, J. N. Shen and J. Wang, *Chin. J. Cancer*, 2011, **30**, 426-432.